

## **A Numerical Study on the Influence of Aggregate Size on Skid Resistance Performance of Porous Pavements**

Lei ZHANG <sup>a</sup>, Ghim Ping ONG <sup>b</sup>, Tien Fang FWA <sup>c</sup>

<sup>a,b,c</sup> *Department of Civil and Environmental Engineering, National University of Singapore, 117576, Singapore*

<sup>a</sup> *E-mail: a0068326@nus.edu.sg*

<sup>b</sup> *E-mail: ceeongr@nus.edu.sg*

<sup>c</sup> *E-mail: ceefwatf@nus.edu.sg*

**Abstract:** Porous pavements are often used as a means to improve skid resistance during wet weather. During the design and construction phases, porosity is often used as the single parameter representing porous pavement drainage capacity. However it is insufficient to use this parameter to predict frictional performance on porous pavements since pavement mix with different aggregate sizes and yet having identical porosity values can yield significantly different skid resistance behaviors. This paper therefore presents a numerical framework to analyze the influence of aggregate size on porous pavement skid resistance. It was found that despite having identical porosity, pavement mix with larger aggregates can provide higher permeability value which consequently reduces the water film thickness on pavement surface under a given rainfall intensity and relieves the hydrodynamic pressure build-up underneath the tire. Porous pavements constructed with larger-size aggregates for a given porosity are found to exhibit better skid resistance performance.

*Keywords:* Skid resistance, Porous pavement, Aggregate size, Computational fluid dynamics, Pore network structure, Water film thickness

### **1. INTRODUCTION**

Highway accidents have posed a tremendous negative effect on society. The World Health Organization (WHO) reported that the worldwide motor vehicle crashes resulted in 1.2 million fatalities and 50 million injuries annually, with an estimated economic loss of US\$518 billion (Peden et al., 2004). It was further found in other studies that a large percentage of accidents on highways happen as a result of unsatisfactory wet-pavement skid resistance performance. For example, Dahir and Gramling (1990) found that 13.5% of fatal crashes and 18.8% of all crashes in the United States occurred on wet pavements. Roe et al. (1991) compared wet-pavement skid resistance data, road surface texture information and accident data for roads in Britain and found that there was a strong correlation showing that accident risk increases with decreasing skid resistance. In a recent study, McGovern et al. (2011) observed that 70% of the wet pavement crashes in the United States can be prevented by improving wet-pavement friction.

Skid resistance is the force developed when a tire prevented from rotating slides on the pavement surface (Highway Research Board, 1972). This term typically refers to the ability of a pavement surface to resist tire sliding in wet conditions because most types of pavements can provide adequate frictional performance in dry conditions (Woodside and Woodward, 2002). Water accumulated on pavement surface in a raining day serves as a lubricant at the tire-pavement interface, resulting in lower skid resistance. Reduced braking force can be

expected, as well as increased braking distance. Moreover, it gets more difficult to maintain direction control at high speed on wet pavement. It is therefore of utmost importance for pavement engineers and researchers to enhance the wet skid resistance on highways in order to obtain a reduction in the risk of wet weather accidents.

Porous pavement, characterized by its high porosity, is found to be an effective measure in enhancing skid resistance in wet weather. Porous asphalt mix, with mostly single-size large aggregates, provides a high percentage of interconnected voids ranging up to 20% by volume (Anderson et al, 1998). Its superiority in wet pavement skid resistance is widely reported in past research works. For example, McGhee and Clark (2010) compared skid resistance performances of porous friction course (PFC) and stone matrix asphalt (SMA) and found that locked-wheel skid numbers on PFC surfaces were at least 10 SN higher than that on SMA surfaces. Similar conclusions were drawn from field measurements using the dynamic friction tester (Kowalski et al., 2009). In addition to the improved skid resistance at specific test speeds, Isenring et al. (1990) indicated that skid numbers on porous pavements were hardly speed-dependent and skid resistance was well maintained at high speeds.

The superior skid resistance performance of porous pavement is mainly due to its excellent drainage capacity arising from its highly inter-connected pore structure. During the design and construction phases of a porous pavement, porosity typically serves as the control variable in mix design and is assumed to be a surrogate for drainage capacity, while permeability is the functional parameter indicating its drainage properties during road operation. While these two parameters are widely used in practice, neither is a direct indicator of pavement skid resistance. This is further complicated by the fact that for porous mix with different aggregate shapes and sizes but with the same porosity, the porous layer can exhibit different permeability values and skid resistance performances.

Recognizing the need to understand the relationship between porosity, permeability and skid resistance for porous mix with different aggregate shapes and sizes, this paper attempts to investigate the influence of aggregate size on skid resistance of porous pavements from a theoretical-numerical perspective. The developed analytical framework consists of three modules, a permeability derivation module, a water film thickness computation module and a skid resistance simulation module. After the detailed explanations of each module, this framework is used in an illustrative case study to quantitatively analyze the skid resistance of various porous pavements with identical porosity value but different aggregate sizes.

## **2. DEVELOPMENT OF ANALYSIS FRAMEWORK**

Figure 1 shows the proposed analysis framework to determine skid resistance on porous pavements under a given set of vehicle operating and environmental conditions. The first step in the analysis framework is the analysis of drainage properties in the porous mixture. Permeability is commonly used as an indicator of drainage capacity in porous media. Although drainage capacity is directly related to the fraction of connected air voids in the porous mix, experiments have shown that the permeability values of porous pavements with similar porosities vary a lot, in some cases up to 100% difference (Neithalath et al., 2010). A reason for this observation is that aggregate size significantly affects the size of pores and the tortuosity of capillaries within the porous layer, both of which are extremely influential in drainage performance. As such, permeability of a porous pavement layer with a specific porosity value and aggregate size is proposed in our analysis framework to be first derived through numerical simulations of outflow tests.

Permeability derived from the first step serves as input to the second step which is to compute the water film thickness accumulated on the porous pavement surface. The amount of water accumulated on pavement surface is known to have a significant influence on skid resistance (Rose and Gallaway, 1977). Water serves as lubricant at tire-pavement interface when it fails to escape from the contact patch at the instant of tire passing. A larger water film thickness often results in lower skid resistance. The accumulation of rainwater on a porous pavement surface is heavily dependent on the drainage capacity of the pavement (i.e. its permeability) as well as the pavement surface characteristics (such as texture, aggregate patterns and geometries). The thickness of water film on a porous pavement under a given rainfall intensity can be computed in this stage using hydraulic theories.

With known water film thickness as well as permeability of the porous pavement layer, skid resistance on porous pavement can be determined through a finite element simulation model. Standard lock-wheel skid tests are simulated in this model. Simulation conditions are set to actual testing conditions and the skid number is derived as part of the model outputs. Details of the three modules are described in the following subsections.

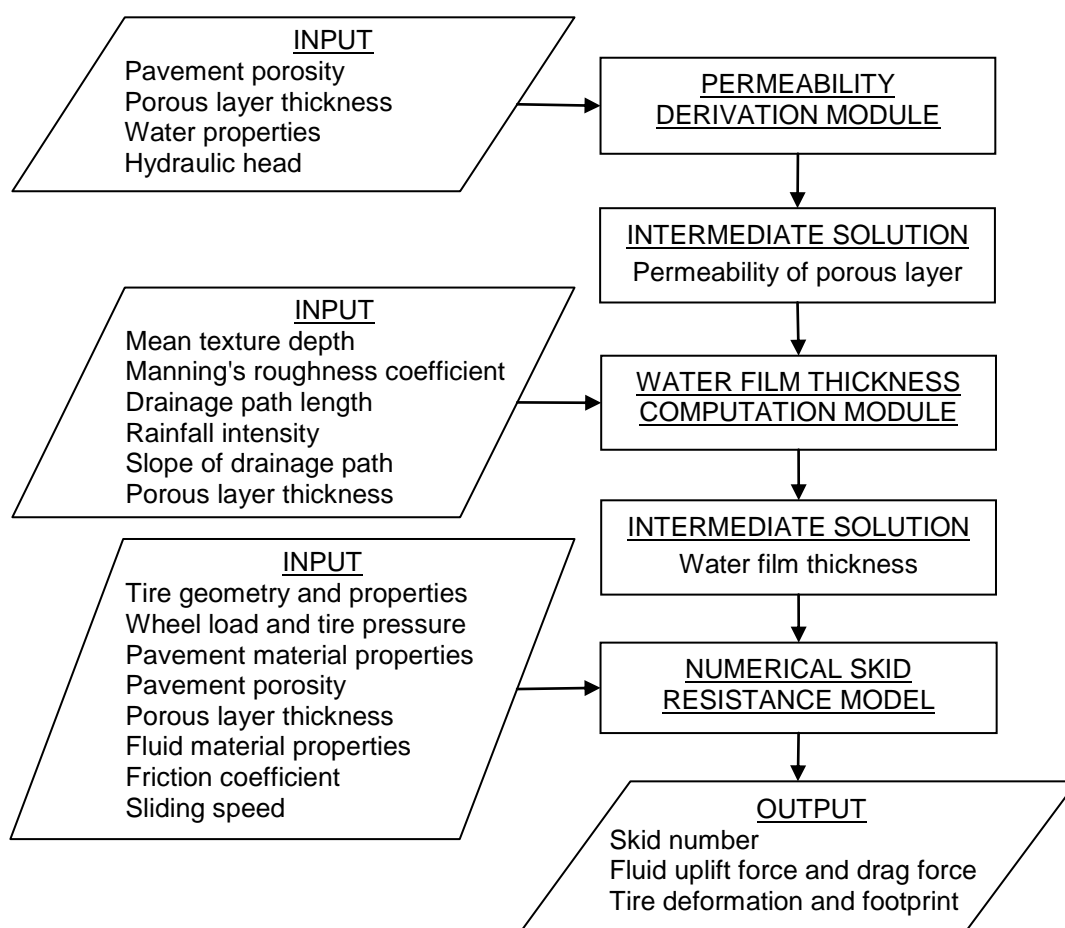


Figure 1. Framework of analytical determination of skid resistance on porous pavement

## 2.1 Permeability Derivation Module

Permeability is a measure of the ability of a porous material to allow fluids to pass through it, and hydraulic conductivity is a material property that describes the ease which water can move through in pore spaces. In practice, it is more convenient to measure hydraulic conductivity through a constant-head or falling-head outflow test and then convert the result

to a permeability value. The relationship between permeability ( $\kappa$ ) and hydraulic conductivity ( $k$ ) is

$$\kappa = k \frac{\mu}{\rho g} \quad (1)$$

where,

$\mu$ : fluid dynamic viscosity,

$\rho$ : fluid density, and

$g$ : acceleration due to gravity.

Hydraulic conductivity for non-Darcy flow can be derived from the heuristic correlation:

$$v = ki^m \quad (2)$$

where,

$i$ : hydraulic gradient,

$k$ : pseudo hydraulic conductivity, and

$m$ : flow condition index (value in range of 0.5 to 1).

Apply the natural logarithm to Equation (2):

$$\ln(v) = \ln(k) + m \ln(i) \quad (3)$$

Noting that  $i = h / l$  (where  $h$  is the hydraulic head and  $l$  is the thickness of the porous specimen), values of  $v$  and  $i$  can be derived from falling-head or constant-head outflow test data. Permeability  $k$  can then be obtained through linear regression.

In this analytical framework, outflow tests are simulated by finite volume method. A grid pore-network model was developed and validated in the authors' previous work (Zhang et al. 2012). This model was proven to be adequate for permeability modelling applications and was successfully adopted to analyze the influence of aggregate size on pavement permeability (Zhang et al. 2013). Connected air voids within the porous pavement are simplified in the model as straight channels in the longitudinal, transverse and vertical directions (Figure 2-a), with a cubic pore element spatially repeated in all three directions (Figure 2-b). The edge length of each drainage channel ( $x$ ) and the distance between centres of two successive parallel channels ( $y$ ) are calibrated to specify the pore network structure. In this model, the spacing of successive channels represents the nominal aggregate size in porous mixture.

Water flow condition in porous pavement layer is closer to turbulence (Chuai, 1998). Therefore,  $k$ - $\varepsilon$  turbulence model is adopted to consider the turbulence effects. The continuity and momentum equations are defined as:

$$\frac{\partial \rho}{\partial t} + \nabla \cdot (\rho U) = 0 \quad (4)$$

$$\frac{\partial \rho U}{\partial t} + \nabla \cdot (\rho U \otimes U) = -\nabla p' + \nabla \cdot (\mu_{eff} (\nabla U + (\nabla U)^T)) + S_M \quad (5)$$

where,

$S_M$  = sum of body forces,

$$p' = \text{modified pressure} = p + \frac{2}{3} \rho k + \frac{2}{3} \mu_{eff} \nabla U, \text{ and}$$

$$\mu_{eff} = \text{effective viscosity} = \mu + \mu_t.$$

The turbulence viscosity  $\mu_t$  is calculated by:

$$\mu_t = C_\mu \rho \frac{k^2}{\varepsilon} \tag{6}$$

where,

$k$  = turbulence kinetic energy,

$\varepsilon$  = turbulence eddy dissipation, and

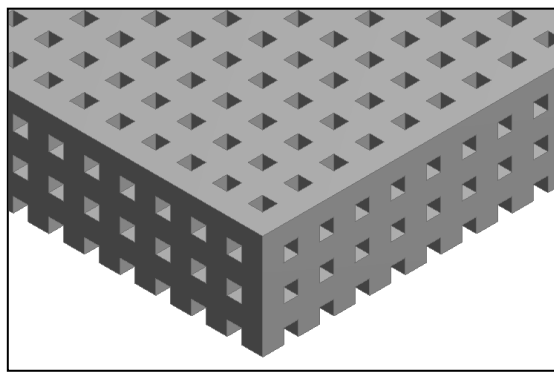
$C_\mu$  = model constant.

The values of  $k$  and  $\varepsilon$  come directly from the differential transport equations:

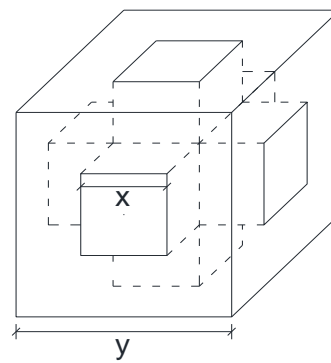
$$\frac{\partial(\rho k)}{\partial t} + \nabla \cdot (\rho U k) = \nabla \cdot \left[ \left( \mu + \frac{\mu_t}{\sigma_k} \right) \nabla k \right] + P_k + P_{kb} - \rho \varepsilon \tag{7}$$

$$\frac{\partial(\rho \varepsilon)}{\partial t} + \nabla \cdot (\rho U \varepsilon) = \nabla \cdot \left[ \left( \mu + \frac{\mu_t}{\sigma_\varepsilon} \right) \nabla \varepsilon \right] + \frac{\varepsilon}{k} (C_{\varepsilon 1} (P_k + P_{\varepsilon b}) - C_{\varepsilon 2} \rho \varepsilon) \tag{8}$$

where  $C_{\varepsilon 1}$ ,  $C_{\varepsilon 2}$ ,  $\sigma_k$  and  $\sigma_\varepsilon$  are model constants,  $P_{kb}$  and  $P_{\varepsilon b}$  represent buoyancy turbulence, and  $P_k$  is the turbulence production due to viscous forces.



(a) Geometry of porous pavement layer



(b) Cubic pore element

Figure 2. Pore network structure of porous pavement model

## 2.2 Water Film Thickness Computation Module

The thickness of water film accumulated on its surface under a given rainfall intensity is related to its drainage capacity. Numerous past research studies had attempted to analyze the drainage characteristics of porous pavements and various methods had been developed to compute the amount of water film thickness accumulated on porous pavements for a given rainfall (Ranieri et al., 2012). Whilst any of these methods developed in past research studies can be applied for this module, this paper adopts the computation model developed by

Anderson et al. (1998) for its simplicity and ease of implementation. In this model, water film thickness accumulated on pavement surface is computed using Equation (9):

$$t_w = \left[ \frac{nL(i-f)}{\alpha S^{0.5}} \right]^{0.6} - MTD \quad (9)$$

where,

- $t_w$  : water film thickness (mm),
- $n$  : Manning's roughness coefficient,
- $L$  : drainage path length (m),
- $i$  : rainfall intensity (mm/h),
- $f$  : infiltration rate into the porous pavement (mm/h),
- $\alpha$  : model constant
- $S$  : slope of drainage path (m/m), and
- MTD: mean texture depth (mm).

Manning's roughness coefficient accounts for the hydraulic effect of pavement surface on surface water flow and its value is surface-dependent. Anderson et al. (1998) in their experimental studies had derived the Manning's coefficients for common asphalt and concrete pavement surface types and these values are used in the paper. The infiltration rate of porous pavement is related to its maximum drainability (Charbeneau and Barrett, 2008) and can be estimated using Equation (10):

$$f = \frac{khS}{L} \quad (10)$$

where,

- $k$  : hydraulic conductivity of the porous layer (mm/h), and
- $h$  : porous layer thickness (m).

Equations (9) and (10) are incorporated into the PAVDRN software (Anderson et al. 1998). For a given rainfall intensity, roadway geometry and porous pavement properties, the water film thickness accumulated on porous pavement surface can be computed using PAVDRN.

### 2.3 Skid Resistance Simulation Model

A mechanistic evaluation of skid resistance on flooded porous pavements would ideally consider the pavement drainage properties, tire structural mechanics, tire-pavement contact, fluid dynamics and tire-fluid interaction. Three-dimensional skid resistance models capable to model these intricate tire-fluid-pavement interactions have been previously developed by the authors to simulate skid resistance and hydroplaning on wet porous and non-porous pavement surfaces (Ong and Fwa, 2007; Zhang et al., 2013). The pivotal considerations in these models are briefly introduced here.

An illustration of the numerical simulation model of skid resistance on porous pavement is shown in Figure 3. A locked wheel skidding on a flooded porous pavement under specific conditions is simulated in the model to replicate the standard lock-wheel skid test (ASTM, 2006). The wheel is stationary in this frame of reference with the pavement, air and water moving at sliding speed towards the wheel.

The skid resistance simulation model consists of three major components: (1) pneumatic tire sub-model, (2) multiphase fluid sub-model and (3) porous pavement sub-model. The sub-models interact with each other either through fluid-structure-interaction or tire-pavement contact algorithm. The frictional contact condition as well as the fluid uplift force and drag force can be computed from this model, if proper information in properties of tire, fluid and pavement are provided.

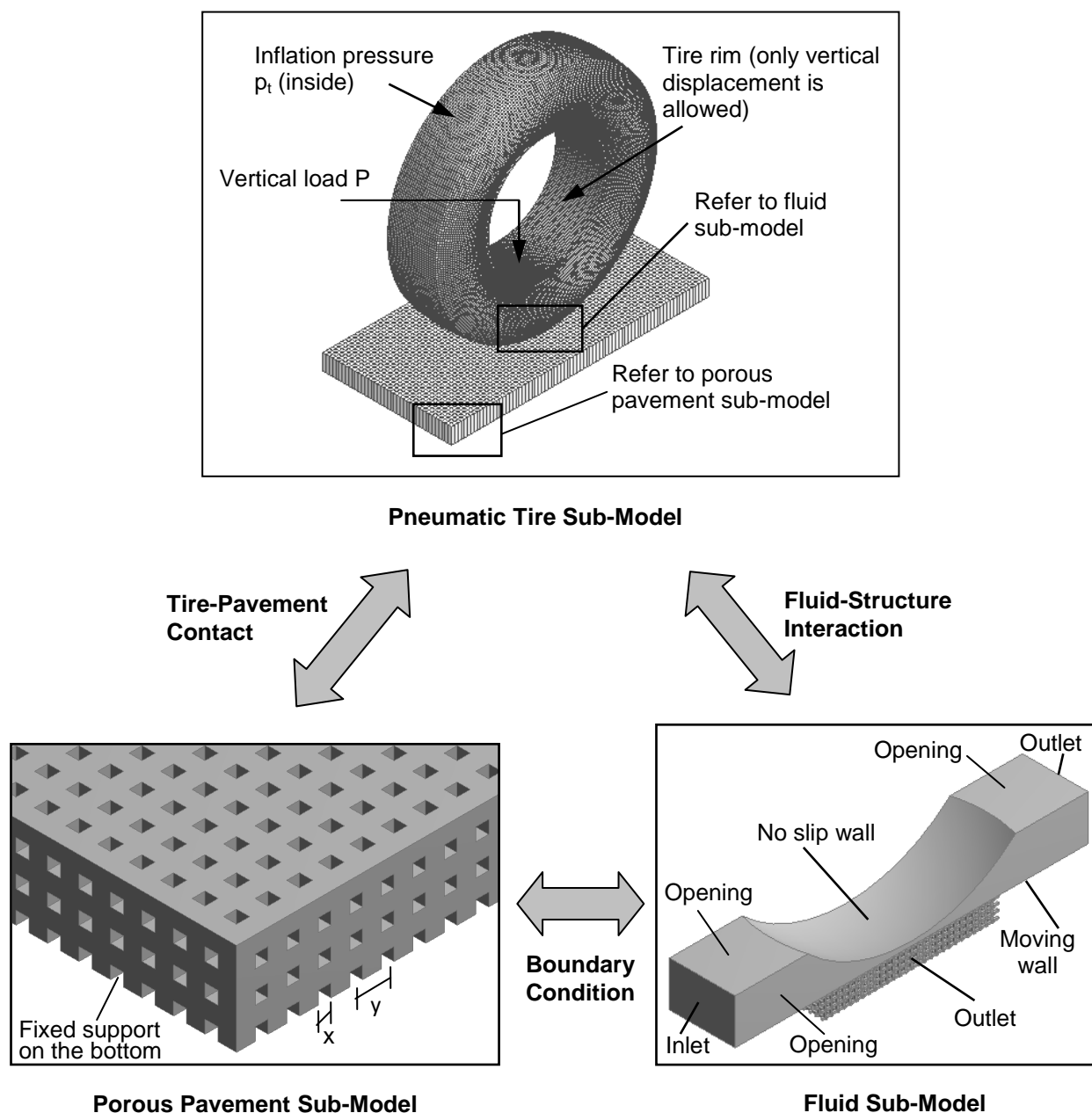


Figure 3. Skid resistance simulation model

ASTM E524 tire (ASTM, 2008) is modeled as the standard test tire. Three structural components, namely the tire rim, tire sidewalls and tire tread are being individually modeled. Contact between tire tread and pavement surface is assumed to follow the Coulomb's concept of friction. Four-node finite strain shell elements are adopted to model the tire components.

Tire material properties are calibrated through comparison against published experiments and differences in contact footprints are taken as the convergence criterion.

Fluid behavior is modeled through the full Navier-Stokes equations. The standard k-ε model (Equations 4 to 8) is adopted for modeling turbulent flow around the tire and inside porous layer. A multiphase flow approach is also adopted for the fluid sub-model, where both air and water are taken into consideration to better reproduce the actual tire-fluid-pavement interaction. The free surface between air and water is captured by volume-of-fluid (VOF) method. Standard properties of water and air at 25°C are adopted in this paper. Mesh convergence study showed that approximately 3.2 million fluid elements are required to produce accurate and reliable results.

The pavement sub-model serves two functions. First, it provides a rigid surface for tire-pavement contact. For this purpose, the pavement surface can be assumed to be perfectly flat and rigid. Second, the pavement sub-model allows for the modeling of fluid flow within the porous layer. In this case, it is necessary to model the effect of pore structure on drainage capacity of the porous pavement within the sub-model. The simplified pore network structure shown in Figure 2 is adopted for this purpose.

The skid number at speed  $v$  ( $SN_v$ ) is determined from the simulation model from Equation (11):

$$SN_v = \frac{F_x}{F_y} \times 100 = \left[ \frac{F_t + F_d}{F_z} \right] \times 100 = \left[ \frac{\mu(F_z - F_u) + F_d}{F_z} \right] \times 100 \quad (11)$$

where,

- $F_x$  : total resisting forces acting on the wheel,
- $F_t$  : traction force,
- $F_z$  : vertical wheel load,
- $F_u$  : fluid uplift force,
- $F_d$  : fluid drag force, and
- $\mu$  : friction coefficient of tire-pavement interface.

### 3. APPLICATION OF THE FRAMEWORK TO ANALYZE THE INFLUENCE OF AGGREGATE SIZE ON SKID RESISTANCE OF POROUS PAVEMENTS

For porous mix design, porosity is usually taken as the sole parameter indicating the potential drainage capacity of the porous layer and as well as predicting its potential skid resistance performance during operations. Porosity is a simple volumetric parameter showing the content of voids in percentage of total mixture volume. It is insufficient to rely only on porosity value as the size and shape of pores as well as their connectivity have significant influence on drainage properties and skid resistance. The variation of pore configuration is mainly determined by the aggregate size and shape. The nominal aggregate size can be taken as an indirect indicator of the pore configuration because single size aggregates from the same source are normally used in the mixture design of the porous layer.

A case study is presented in this paper using the developed analysis framework to quantify and compare skid resistance performances of porous pavements with identical porosity but various aggregate sizes. As a simplification, the case study presented in this paper considers a two-way four-lane tangent section of 15-m road width and a 2% cross-slope. A 50 mm thick porous asphalt surface layer with 20% porosity is planned to be laid on an

impermeable dense graded asphalt base course. The skid resistance performances of three mixtures are to be predicted and examined during the design phase using the analysis framework presented in the paper.

The nominal aggregate sizes of the three porous mixes are 12 mm, 16 mm and 20 mm respectively. All three mixes use aggregate and asphalt from the same sources so that the inherent friction coefficients at tire-pavement interface can be assumed to be the same. This inherent friction coefficient is assumed to take a value of 0.50. Skid number (SN) [as defined in ASTM (2006)] is used as a measure of pavement skid resistance. Numerical simulation of the locked wheel friction tests are performed under different vehicle speeds (40 km/h, 60 km/h and 80 km/h) and rainfall intensities (60 mm/h, 150 mm/h and 300 mm/h).

### 3.1 Permeability Values

To represent the pore structure of an actual porous pavement with the grid network shown in Figure 2, shapes of aggregates and pores are simplified as shown in Figure 4. In this reduced model, for a specific porosity value  $\phi_0$ , the constant ratio between pore size  $x$  and aggregate size  $y$  ( $x/y = c$ ) can be derived in Equation (12).

$$\phi_0 = \frac{V_{pore}}{V_{total}} = \frac{3x^2y - x^3}{y^3} = c^2(3 - c) \quad (12)$$

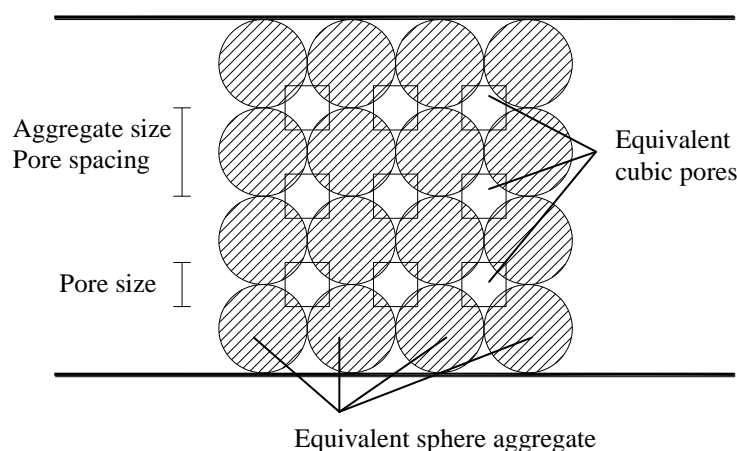


Figure 4. Simplified representation of porous layer structure

The permeability values of the three mixtures are first derived by numerical simulations of constant-head outflow tests. The diameter of outflow meter is assumed to be 150 mm. The geometry parameters of each mixture design are calculated from Equation (10) and are shown in Table 1. For each mix, numerical simulation of the constant-head outflow test were performed using five hydraulic heads (200 mm, 300 mm, 400 mm, 500 mm and 600 mm). The mass flow rate was monitored as the direct output and permeability value were computed. Permeability results from the numerical simulation are also shown in Table 1. It is seen from the table that aggregate size affects permeability of porous pavements despite having the same porosity value. Also, using larger aggregates in the porous mix tends to result in the layer having a higher permeability value.

Table 1. Geometry parameters and permeability values

Porosity (%)	$c=x/y$	Aggregate size (mm)	Pore size (mm)	Permeability ( $m^2$ )
20	0.271	12	3.25	4.533
		16	4.34	4.848
		20	5.42	5.354

### 3.2 Water Film Thickness

The permeability values of the three different mixes as shown in Table 1 allow the computation of the amount of water film thickness accumulated on the porous pavement surfaces under different rainfall intensity conditions. The water film thicknesses are computed using the PAVDRN software (Anderson et al., 1998) and the results are shown in Figure 5. It can be seen from the figure that water film thickness increases as the rainfall intensity increases. More importantly, water film thickness is higher for pavement with smaller aggregates (i.e. lower permeability value) under the same rainfall intensity. The differences in water film thickness between different aggregate sizes are found to be more discernible at lower rainfall intensities, but marginal at higher rainfall intensities. This observation indicates that the efficiency of water film thickness reduction on porous pavements is related to aggregate size and may have an impact on skid resistance performance.

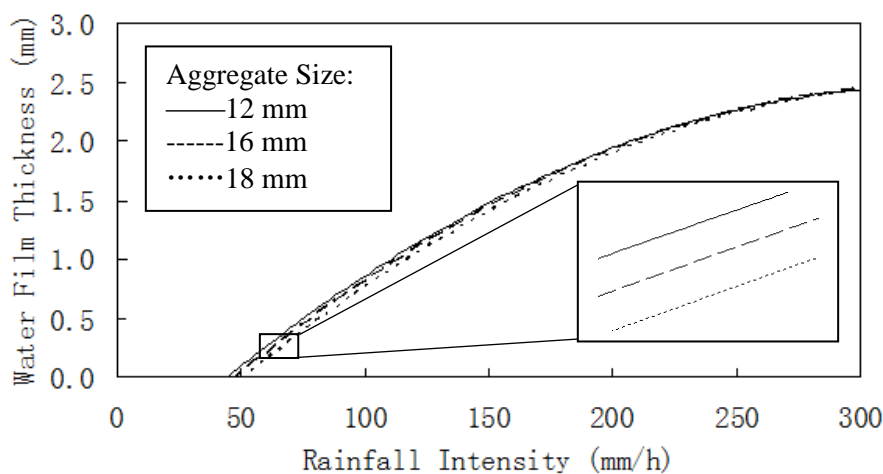
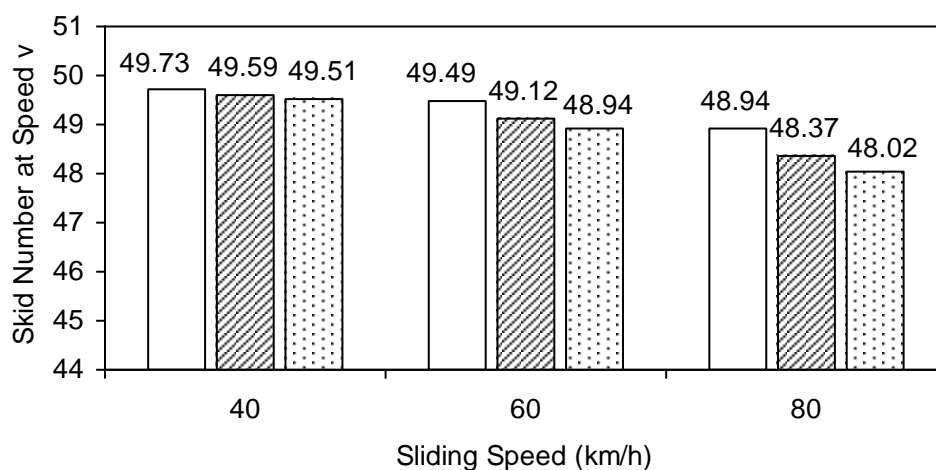


Figure 5. Comparison of water film thicknesses on different porous pavements

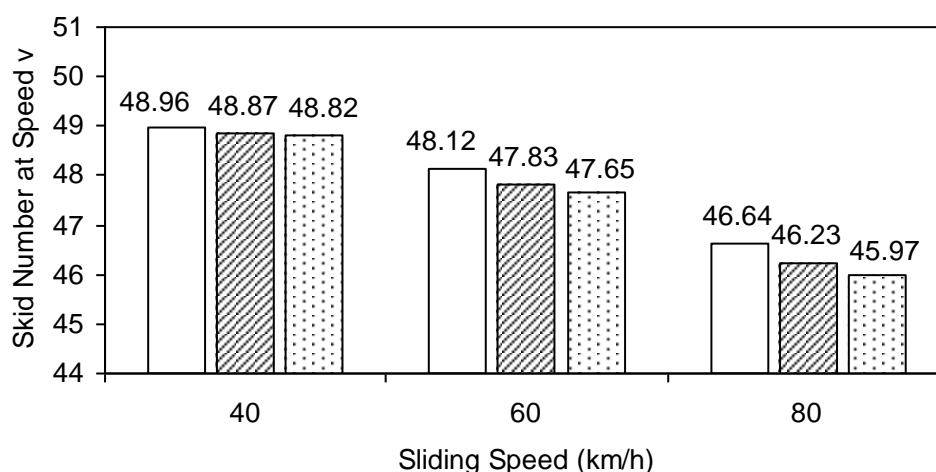
### 3.3 Skid Number at Specific Speed

The water film thicknesses computed earlier in Figure 5 serves as an input to the skid resistance simulation model. Standard locked-wheel skid tests (ASTM, 2006) are simulated on the three porous layers with different aggregate sizes defined in this case study and skid numbers are derived from model outputs. The results are shown in Figure 6, from which the following observations can be made:

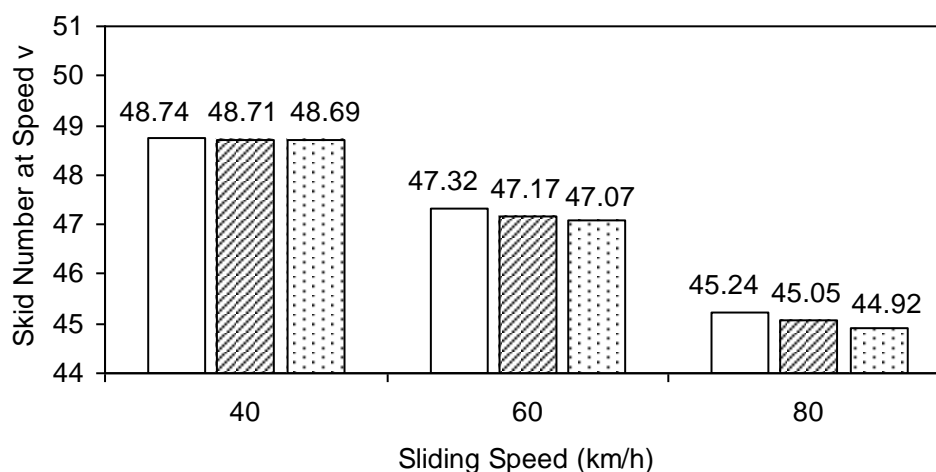
- For porous pavements with identical porosity, skid number increases with an increase in aggregate size at the same rainfall intensity and sliding speed. The differences are less significant at lower speeds, and more significant at higher speeds. In the case study, the skid number is improved by 1.9% at 80 km/h sliding speed and



(a) 60 mm/h Rainfall Intensity



(b) 150 mm/h Rainfall Intensity



(c) 300 mm/h Rainfall Intensity

Aggregate Size: □ 20 mm ▨ 16 mm ▩ 12 mm

Figure 6. Skid resistance performances of three porous pavements at different sliding speeds

60 mm/h rainfall intensity, if the nominal aggregate size in mixture design increases from 12 mm to 20 mm.

- Skid resistance performance for a specific porous pavement decreases with increasing sliding speed and rainfall intensity. For the case of 12 mm aggregate size and 300 mm/h rainfall intensity, skid number is reduced by 8.4% when the sliding speed increases from 40 km/h to 80 km/h. For the case of 20 mm aggregate size and 80 km/h sliding speed, skid number is reduced by 8.4% when the rainfall intensity is increased from 60 mm/h to 300 mm/h.
- Porous surface layer significantly enhances wet-pavement skid resistance to the point that skid number still remains higher than the requirement of 35 recommended for heavily traveled road (Jayawickrama et al., 1996) at the condition of 12 mm aggregate size, 300 mm/h rainfall intensity and 80 km/h sliding speed.

From the above observations, it was found that aggregate size does have an influence on the skid resistance performance of porous pavements with identical porosity. However, this influence is not critical in the normal practical range because the overall frictional properties are maintained well on porous pavements.

#### 4. CONCLUSION

Understanding that porous pavements with identical porosity value may exhibit different skid resistance performances (a result of the different aggregate sizes used in the mix design), this study developed an analysis framework to evaluate the influence of aggregate size on skid resistance performance of porous pavements. The proposed framework consists of three previously-developed sub-modules, from which the permeability of porous layer, the water film thickness on pavement surface, and the skid number in standard skid test are derived sequentially. The applicability of this framework is demonstrated through a case study analyzing the skid resistance performances of three porous surface layers with different aggregate sizes. It was found from the case study that porous pavement constructed by larger aggregates can provide higher drainage capacity through a larger permeability value, despite having the same porosity. This property helps reduce the water film thickness under a given rainfall intensity and increase the skid number of the pavement surface. The findings obtained in this work should be examined through field experiments before solid conclusions can be integrated into the design and management of porous pavements. Parametric studies could be conducted to improve the skid resistance performance of porous pavements more efficiently.

#### REFERENCES

- Anderson, D.A., Huebner, R.S., Reed, J.R., Warner, J.C., Henry, J.J. (1998) *Improved Surface Drainage of Pavements*. National Cooperative Highway Research Program Project 1-29, Pennsylvania State University, Pennsylvania.
- ASTM. (2006) Standard Test Method for Skid Resistance of Paved Surfaces Using a Full-Scale Tire. ASTM Standard E274-06, American Society for Testing and Materials, Pennsylvania.
- ASTM. (2008) Standard Specification for Standard Smooth Tire for Pavement Skid-Resistance Tests. ASTM Standard E524-08, American Society for Testing and Materials, Pennsylvania.
- Charbeneau, R.J., Barrett, M.E. (2008) Drainage Hydraulics of Permeable Friction Courses. *Water Resources Research* (44).

- Chuai, C.T. (1998) *Measurement of Drainage Properties of Porous Asphalt Mixtures*. Ph.D. Thesis, National University of Singapore, Singapore.
- Dahir, S.H., Gramling, W.L. (1990) *Wet Pavement Safety Programs*. National Cooperative Highway Research Program Synthesis of Highway Practice 158, Transportation Research Board, Washington, D.C.
- Highway Research Board (1972) *Skid Resistance*. National Cooperative Highway Research Program Synthesis of Highway Practice, No. 14, Highway Research Board, Washington D.C.
- Isenring, T., Koster, H., Scazziga, I. (1990) Experiences with Porous Asphalt in Switzerland. *Transportation Research Record*, No. 1265, 41-53.
- Jayawichrama, P.W., Prasanna, R., Senadheera, S.P. (1996) Survey of State Practices to Control Skid Resistance on Hot-Mix Asphalt Concrete Pavements. *Transportation Research Record*, No. 1536, 52-58.
- Kowalski, K., McDaniel, R.S., Shah, A., Olek, J. (2009) Long term monitoring of the noise and frictional properties of three pavements: dense-graded asphalt, stone matrix asphalt, and porous friction course. *Transportation Research Record*, No. 2127, 12-19.
- McGhee, K.K., Clark, T.M. (2010) Functionally optimized wearing course: installation report. *Transportation Research Record*, No. 2180, 150-155.
- McGovern, C., Rusch, P., Noyce, D.A. (2011) *State Practices to Reduce Wet Weather Skidding Crashes*. Publication FHWA-SA-11-21. Federal Highway Administration, U.S. Department of Transportation, Washington, D.C.
- Neithalath, N., Sumanasooriya, M.S., Deo, O. (2010) Characterizing pore volume, size, and connectivity in pervious concretes for permeability prediction, *Materials Characterization*, 61, 802-812.
- Ong, G.P., Fwa, T.F. (2007) Wet-Pavement Hydroplaning Risk and Skid Resistance: Modeling. *Journal of Transportation Engineering*, 133(10), 590-598.
- Peden, M., Scurfield, R., Sleet, D., Mohan, D., Hyder, A., Jarawan, E., Mathers, C. (2004) *World Report on Road Traffic Injury Prevention*. World Health Organization, Geneva.
- Ranieri, V., Ying, G., Sansalone, J. (2012) Drainage Modeling of Roadway Systems with Porous Friction Courses. *Journal of Transportation Engineering*, 138 (4), 395-405.
- Roe, P.G., Webster, D.C., West, G. (1991) *The Relation Between the Surface Texture of Roads and Accidents*. TRRL Research Report 296, Transport and Road Research Laboratory, Berkshire.
- Rose, J.G., Gallaway, B.M. (1977) Water depth influence on pavement friction. *Journal of Transportation Engineering*, 103(4), 491-506.
- Woodside, A.R., Woodward, W.D.H. (2002) Wet skid resistance. In O'Flaherty, C.A. (eds.), *Highways: The Location, Design, Construction and Maintenance of Road Pavements*, 4th edition, 479-499. Butterworth Heinemann, Oxford.
- Zhang, L., Ong, G.P., Fwa, T.F. (2012) Three dimensional modeling of porous pavement permeability using a simplified pore network structure, Proceedings of the 7th International Conference on Maintenance and Rehabilitation of Pavements and Technological Control, Auckland, New Zealand.
- Zhang, L., Ong, G.P., Fwa, T.F. (2013) Developing an analysis framework to quantify and compare skid resistance performances on porous and non-porous pavements. Proceedings of the the 92nd Transportation Research Board Annual Meeting, Washington, D.C., United States.
- Zhang, L., Ong, G.P., Fwa, T.F. (2013) Evaluating the influence of aggregate size on permeability of porous pavements using finite volume simulation. Proceedings of the

8th International Committee on Road and Airfield Pavement Technology, Taipei, Taiwan.